# Design and Fabrication of Electrospun Polyethersulfone Nanofibrous Scaffold for High-Flux Nanofiltration Membranes

ZHAOHUI TANG,[1] CHANGQUAN QIU,[2] JEFFREY R. McCUTCHEON,[3] KYUNGHWAN YOON,[2] HONGYANG MA,[2] DUFEI FANG,[2] ERIC LEE,[4] CLINT KOPP,[4] BENJAMIN S. HSIAO,[2] BENJAMIN CHU[2]

[1]State Key Laboratory of Polymer Physics and Chemistry, Changchun Institute of Applied Chemistry, Chinese Academy of Sciences, Changchun 130022, China

[2]Department of Chemistry, Stony Brook University, Stony Brook, New York 11794-3400

[3]Department of Chemical, Materials and Biomolecular Engineering, University of Connecticut Storrs, Connecticut 06269-3222

[4]Stonybrook Purification, Inc., Stony Brook University, Stony Brook, New York 11794-3400

*Received 7 May 2009; revised 7 July 2009; accepted 16 August 2009*
*DOI: 10.1002/polb.21831*
*Published online in Wiley InterScience (www.interscience.wiley.com).*

**ABSTRACT:** A novel class of high-flux and low-fouling thin-film nanofibrous composite (TFNC) membranes, containing a thin hydrophilic top-layer coating, a nanofibrous mid-layer scaffold and a non-woven microfibrous support, has been demonstrated for nanofiltration (NF) applications. In this study, the issues related to the design and fabrication of a polyethersulfone (PES) electrospun nanofibrous scaffold for TFNC NF membranes were investigated. These issues included the influence of solvent mixture ratio, solute concentration, additives, relative humidity (RH), and solution flow rate on the morphology of an electrospun PES nanofibrous scaffold, the distribution of fiber diameter, the adhesion between the PES scaffold and a typical poly(ethylene terephthalate) (PET) non-woven support, as well as the tensile properties of the nanofibrous PES/non-woven PET composite substrates. Uniform and thin nanofibrous PES scaffolds with strong adhesion to the nanofiber-PET non-woven are several of the key parameters to optimize the NF performance of TFNC membranes.
© 2009 Wiley Periodicals, Inc. J Polym Sci Part B: Polym Phys 47: 2288–2300, 2009
**Keywords:** adhesion; electrospinning; filtration; membranes; nanocomposites; nanofiber; polyethersulfone

## INTRODUCTION

Nanofiltration (NF) is a pressure-driven membrane process for liquid separation.[1] NF is typically used in treatment processes that require more selectivity than ultrafiltration (UF), but less than reverse osmosis (RO),[2,3] hence NF is essentially a low-pressure RO.[4] NF membranes typically have more high-flux at low pressures, when compared with RO membranes but are still effective at removing some salts, bacteria, viruses, pesticides, and other organic contaminants from surface water and fresh groundwater. As such, NF is suitable for the treatment of surface water and well water to produce and, in

*Correspondence to:* B. S. Hsiao (E-mail: bhsiao@notes.cc.sunysb.edu) or B. Chu (E-mail: bchu@notes.cc.sunysb.edu)
Journal of Polymer Science: Part B: Polymer Physics, Vol. 47, 2288–2300 (2009)
© 2009 Wiley Periodicals, Inc.

some cases, soften public drinking water.[5–7] Because NF runs under lower pressure than RO, energy costs are lower than a comparable RO system.

Most commercial NF membranes are thin-film composite (TFC) membranes.[8–10] TFC NF membranes are typically made by forming an ultra-thin selective barrier layer on a porous support layer through interfacial polymerization of a poly-functional amine with a poly-functional acyl chloride. The properties of this ultra-thin selective barrier layer have a crucial influence on the performance of TFC NF membranes, such that a significant number of investigations have focused on the optimization of the selective barrier layer.[11–17] Asymmetric polymeric membranes, made from casting polysulfone,[9] polyethersulfone (PES),[18] polyacrylonitrile,[19,20] poly(vinylidene fluoride),[17] polypropylene,[21] or polyimide,[22] can be used as a porous support substrate to make TFC membranes. The porous support provides mechanical stability and allows the application of an ultra-thin and defect-free selective barrier top layer.[2] However, the casting method of the polyamide layer may result in pores being collapsed in the porous support layer at the interface, resulting in a decrease of flux of TFC membranes.[2,23,24] The characteristics of porous support layers can impact this phenomenon and hence can affect not only the flux but also the rejection ratio of TFC membranes.[25] As such, the choice of a porous support becomes important.

Electrospinning is a method of polymer processing that is gaining attention in the academic and industrial worlds. This fabrication technique is capable of producing polymeric fibers with diameters ranging from <100 nm to several microns. The non-woven structures that are created by electrospinning typically exhibit extremely high surface and bulk porosity and contain very open interconnected (down to sub-micron diameter pores, depending on fiber diameter and porosity) pore structures.[26–28] The porosity of the electrospun scaffold can reach >90%.[29] This high porosity makes the electrospun scaffold a good candidate for air and liquid filtration.[30] In particular, the Chu/Hsiao group has recently developed high-flux thin-film nanofibrous composite (TFNC) membranes based on electrospun nanofiber/poly(ethylene terephthalate) (PET) non-woven composite substrates, suitable for both UF and NF.[31–34] The TFNC membranes exhibited superior flux over commercial flat sheet membranes.

For a useable TFNC membrane, the adhesion of the electrospun nanofibers to the PET non-woven support is critical. Weak adhesion will lead to delamination during membrane handling or operation. The uniform porosity and fiber diameter distributions as well as the small-fiber diameter are the key factors that ensure the casting of a thin and uniform selective barrier layer on top of the nanofibrous scaffold. In this investigation, we report on the design and fabrication of the electrospun PES nanofiber/PET (nano-PES/PET) non-woven composite substrates. PES was used as the material for making the electrospun nanofiber, as it is widely used as a membrane support material due to its outstanding chemical resistance and thermal stability.[35,36] It should be noted that variation in the physio–chemical properties of the materials used in the electrospinning process also changes the required processing conditions.

## EXPERIMENTAL

### Materials

Polyethersulfone (PES, RADEL H-3000, $M_w$ 7.8 × $10^4$, $M_n$ 2.5 × $10^4$, $M_w/M_n$ 3.1) was obtained from Solvay Advanced Polymers. PET non-woven support (Sanko 16-1) was obtained from Sanko. PTFE syringe filter (0.45 $\mu$m) was obtained from Fisher Scientific. Dimethylformamide (DMF, 99.9%), *N*-methylpyrrolidone (NMP, 99%), and poly(ethylene oxide) (PEO, $M_w$ 5 × $10^6$) were obtained from Aldrich. The PES was dried at 120 °C under vacuum for 6 h before use. DMF and NMP were dried over molecular sieves (3 Å) before use. Other chemicals were used as received.

### Preparation of PES Solution

PES solutions for electrospinning were prepared by dissolving PES in a mixture of DMF and NMP at a given ratio at 90 °C. The solutions were stirred for 2 days before electrospinning. The composition and viscosity of the PES solution are listed in Table 1.

### Preparation of Electrospun Nanofibrous PES/PET (Nano-PES/PET) Substrate

The nanofibrous PES scaffold was fabricated by electrospinning of PES solution onto a PET non-woven support. The general conditions for electrospinning were as follows: voltage 30 KV;

**Table 1.** Properties of PES Solution

| Solution | PES% (wt/wt) | DMF/NMP (wt/wt) | PEO% (wt/wt) | Viscosity (Pa s) |
|---|---|---|---|---|
| S1 | 22 | 30/70 | 0 | 1.84 |
| S2 | 22 | 40/60 | 0 | 1.71 |
| S3 | 22 | 50/50 | 0 | 1.69 |
| S4 | 22 | 60/40 | 0 | 1.31 |
| S5 | 20 | 60/40 | 0 | 0.69 |
| S6 | 18 | 60/40 | 0 | 0.31 |
| S7 | 20 | 60/40 | 0.5 | 0.89 |

distance between spinneret and rotating drum collector (collector was wrapped with PET non-woven support), 10.5 cm; and temperature, 25 °C. The solutions were filtered with 0.45 $\mu$m PTFE syringe filters immediately before electrospinning.

### Characterization

Viscosity measurements were carried out by a Brookfield viscometer (Model LVTDCP) operating at a shear rate of 0.6 $s^{-1}$ using 0.5 mL solution and at room temperature. The adhesion strength of the PES nanofibrous scaffold to the PET non-woven support was tested by using a Dillon BFG-50N force gauge. The PET non-woven support side of the nanofibrous PES/PET substrate sample (10 mm $\times$ 5 mm) was affixed by a double-faced adhesive tape to a loading fixture (10 mm $\times$ 5 mm). The PES nanofiber side of the nanofibrous PES/PET substrate sample (10 mm $\times$ 5 mm) was affixed by a double-faced adhesive tape to the Dillon BFG-50N force gauge. A load was increasingly applied to the force gauge until the PES nanofiber layer was pulled off. The force required to pull the PES nanofiber layer off was recorded as the adhesion strength of the PES nanofibrous scaffold to the PET non-woven support. The tensile properties of the nano-PES/PET composite substrate were determined by using an Instron (model 4442) tensile machine at ambient temperature. The specimen sizes for the evaluation were 30 mm $\times$ 4 mm $\times$ 120 $\mu$m (length $\times$ width $\times$ thickness). The morphology of the nano-PES/PET composite substrate was characterized by using a LEO 1550 (LEO, USA) scanning electron microscope (SEM) after gold coating of samples. The mean diameter and standard deviation of each electrospun PES sample were calculated from 100 electrospun nanofibers.

## RESULTS AND DISCUSSION

### Electrospinning of PES Nanofiber onto PET Non-Woven Support

The electrospun nanofibrous scaffold is highly porous but its mechanical strength is relatively low. To increase the mechanical strength and handling of the electrospun nanofibrous scaffold, PES was directly electrospun onto the PET non-woven support. Two critical criteria for a serviceable nano-PES/PET composite substrate are (1) adequate adhesion between the PES nanofibrous scaffold and the PET non-woven support as well as (2) the adhesion between the nanofibers themselves. Weakly bonded nanofibers may delaminate significantly during handling or operation. Weak bonding occurs in large part because the PET non-woven fabric is non-conductive and hence tends to collect charge during the electrospinning process. The accumulated charge tends to repel nanofibers from further deposition onto the collector during the electrospinning process. In addition, during the electrospinning process, solvent in the jet stream is being evaporated as the jet stream approaches the collector surface. As most of the solvent is being evaporated during electrospinning, electrospun nanofibers may become too dry when they reach the PET non-woven support. Then, poor adhesion between the nanofibrous mid-layer and the PET non-woven support is likely to occur. If the deposited fiber is wet with solvent, the presence of a small amount of solvent may aid the adhesion to the PET non-woven, especially if PET is partially soluble in the solvent.[37] Second, the nanofibers must adhere strongly to each other within the mid-layer. Weak fiber–fiber bonding results in a soft, "cotton ball"-like material, which is unsuitable for filtration or interfacial polymerization. Strong bonding between the electrospun nanofiber and the PET

non-woven support and between the electrospun fibers themselves are critical for a membrane to be able to withstand changes in cross-flow velocity, hydraulic pressure, and back-flushing. As with improving the PES nanofiber–PET non-woven bonding above, choosing an appropriate solvent system is critical to maximize the nanofiber–nanofiber bonding process. Depositing fibers which are slightly wet may allow nanofibers to form junctions and improve the integrity of the nanofibrous scaffold. We attempted to address both PES nanofiber–PET non-woven and nanofiber–nanofiber bonding problems by adjusting polymer solution properties and the overall electrospinning conditions, which are described as follows. In addition, we have investigated their effects on the porosity and fiber diameter distributions of the nanofibrous scaffolds, which will have direct impact to the ability to support a thin layer of selective barrier layer for water filtration.

### Influence of DMF/NMP Solvent Ratio in Electrospinning of PES

DMF is a commonly used solvent for PES. This solvent evaporates relatively quickly due to a high-vapor pressure at 25 °C (3.85 mmHg).[38] As mentioned earlier, if a solvent evaporates too quickly during electrospinning, the nanofiber may be too dry to allow for adhesion to the non-woven support or adhesion between the nanofibers themselves. *N*-methylpyrrolidone (NMP), another solvent for PES, has a low-vapor pressure at 25 °C (0.5 mmHg at 25 °C)[39] and hence can be mixed with DMF to decrease the evaporation rate. SEM images of the top layer view of nano-PES/PET substrates at different DMF/NMP ratios are shown in Figure 1. Significant nanofiber coalescence appeared in the electrospun web when the DMF/NMP ratio was 30/70 and 40/60 [Fig. 1(a,b)]. This means that the electrospun nanofiber was very wet upon deposition because the presence of NMP had decreased the vapor pressure of the solvent mixture. This led to an excess of solvent on the nanofiber after deposition, resulting in nanofiber dissolution. Film-like structures would actually appear when depositing nanofibers from these "wet" conditions. Nanofibers with much less coalescence were obtained when the DMF/NMP ratio was 50/50 and 60/40 [Fig. 1(c,d)], indicating that the electrospun nanofibers had little or no excess solvent upon reaching the PET non-woven support. In essence, the vapor pressure of the PES solution increased with increasing DMF/NMP ratio, according to, for example, Raoult's law.[40] A wet nanofiber web was obtained when the DMF/NMP ratio was low (e.g., 30/70 and 40/60 ratios). A drier nanofiber web was created when the DMF/NMP ratio was higher (e.g., 50/50 and 60/40 ratios).

It is reasonable to assume that a wet PES nanofibrous scaffold will have stronger adhesion strength to the PET non-woven because of coalescence of electrospun nanofibers. The coalescence will create a large interface region between the PES nanofiber scaffold and the PET non-woven support. As shown in Table 2, the adhesion strength between the nanofiber and the PET non-woven support decreased from 60.8 psi to 0.6 psi as the DMF/NMP ratio increased from 30/70 to 60/40 (Table 2, no. 1–4). Solutions with higher DMF contents resulted in little or no adhesion to the non-woven support. The mean diameter of nanofiber also increased from 126 to 413 nm when the DMF/NMP ratio increased from 30/70 to 60/40 (Table 2, no. 1–4). One possible explanation for this result is the fact that when evaporation of the solvent is faster, the polymer can "precipitate" out of the solution faster. The fiber size decreased during the draw-down process so long as the polymer chains were still at least partially solvated. If the jet stream (fiber) solidified prematurely, then the fiber size became fixed before the jet stream could be adequately stretched out to form a thinner fiber.

The standard deviation of the fiber diameter is represented by the width distribution of the fiber diameter. The standard deviation increased from 36 to 183 nm as the DMF/NMP ratio increased from 30/70 to 60/40 (Table 2, no. 1–4), meaning that an increase in the volatile/low-vapor pressure solvent ratio can lead to a wider distribution of electrospun fiber diameters.

### Influence of PES Concentration in Electrospinning

The diameter of electrospun nanofibers has been shown to increase with increasing polymer concentration.[41–43] It is seen in Table 2 and Figure 2 that as the concentration decreased from 22 wt % to 20 wt %, the nanofibers became thinner but beads began to form within the scaffold. This is a common phenomenon that occurs when the polymer concentration is decreased to below their entanglement concentration or when the viscoelastic properties of the nanofiber favors bead formation. It is important to note, however, that if the polymer solution concentration is decreasing

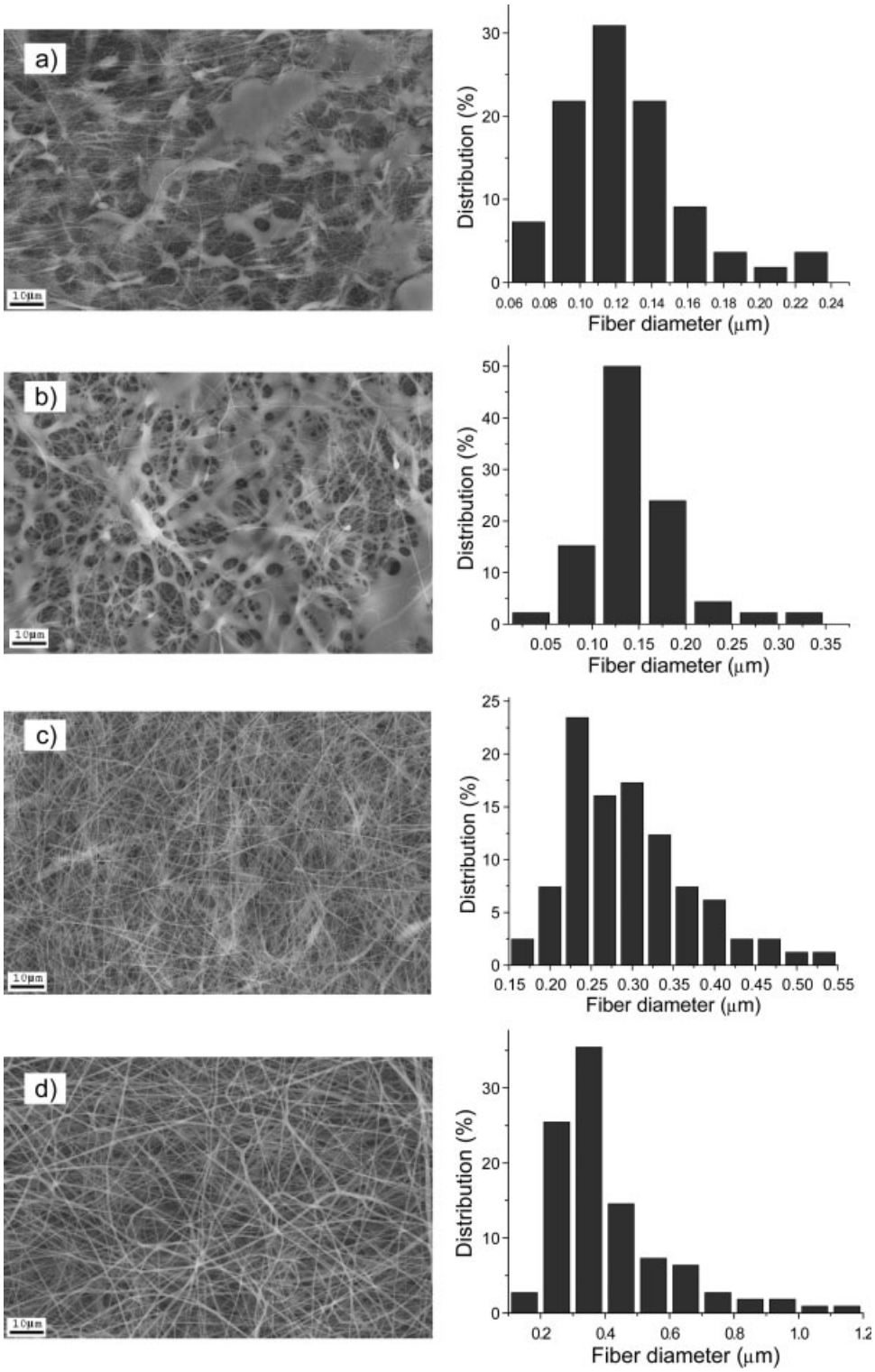


**Figure 1.** SEM images and fiber diameter distribution of electrospun Nano-PES/PET composite substrates fabricated from 22 wt % PES solutions at different DMF/NMP ratio (Table 2, no. 1–4). (a) DMF/NMP = 30/70, mean diameter: 126 nm. (b) DMF/NMP = 40/60, mean diameter: 147 nm. (c) DMF/NMP = 50/50, mean diameter: 298 nm. (d) DMF/NMP = 60/40, mean diameter: 413 nm.

**Table 2.** Electrospinning of PES Solution and Mechanical Properties of Corresponding Nano-PES/PET Composite Substrates[a]

| No. | Sol.[b] | PES% (wt/wt) | DMF/NMP (wt/wt) | RH (%) | Flow Rate ($\mu$L/min) | Dia. (nm)[c] | Adhesion Strength (psi) |
|---|---|---|---|---|---|---|---|
| 1 | S1 | 22 | 30/70 | 50 | 20 | 126 ± 36 | 60.8 |
| 2 | S2 | 22 | 40/60 | 50 | 20 | 147 ± 53 | 52.8 |
| 3 | S3 | 22 | 50/50 | 50 | 20 | 298 ± 78 | 1.2 |
| 4 | S4 | 22 | 60/40 | 50 | 20 | 413 ± 183 | 0.6 |
| 5 | S5 | 20 | 60/40 | 50 | 20 | 329 ± 160 | 34.1 |
| 6 | S6 | 18 | 60/40 | 50 | 20 | 215 ± 134 | 78.7 |
| 7 | S7[d] | 20 | 60/40 | 50 | 20 | 349 ± 160 | 40.2 |
| 8 | S7[d] | 20 | 60/40 | 45 | 20 | 266 ± 81 | 2.6 |
| 9 | S7[d] | 20 | 60/40 | 60 | 20 | 382 ± 164 | 32.0 |
| 10 | S7[d] | 20 | 60/40 | 70 | 20 | 492 ± 211 | 4.7 |
| 11 | S7[d] | 20 | 60/40 | 50 | 15 | 312 ± 112 | 2.6 |
| 12 | S7[d] | 20 | 60/40 | 50 | 25 | 633 ± 267 | 45.3 |
| 13 | S7[d] | 20 | 60/40 | 50 | 30 | 740 ± 408 | 55.1 |
| 14[e] | S7[d] | 20 | 60/40 | 50 | 30/15 | 318 ± 148 | 42.9 |

[a] Electrospinning temperature, 25 °C; voltage, 30 KV; distance between spinneret and PET non-woven substrate, 10.5 cm; thickness of electrospun PES webs, 20 $\mu$m; tensile properties of PET non-woven substrate: tensile modulus 1295 MPa, tensile strength 72.4 MPa, elongation at break 14.2%.
[b] Used solution for electrospinning.
[c] Diameter of electrospun nanofiber = Mean diameter ± Standard deviation.
[d] 20 wt % PES solution with 0.5 wt % PEO additive.
[e] Primer layer: flow rate 30 $\mu$L/min, thickness: 10 $\mu$m; Second layer: flow rate for 15 $\mu$L/min, thickness: 5 $\mu$m.

but the flow rate to the spinneret is remaining the same, more solvent is being delivered over a given time period, which can also have impacts on the scaffold morphology. The low concentration PES solutions, especially the 18 wt %, show extensive coalescence features in Figure 2. The change in the scaffold morphology clearly has an impact on the PES nanofiber–PET non-woven adhesion. For instance, the adhesion strength was 34.1 psi and 78.7 psi, respectively, for 20 wt % and 18 wt % nano-PES/PET substrate (Fig. 6). These values were much higher than that of nano-PES/PET substrate fabricated with the 22 wt % PES solution. The significant enhancement of adhesion could be explained because the wet electrospun scaffold was produced using the low PES solution concentration (20 wt % and 18 wt %). The nanofiber diameter of 20 wt % PES and 18 wt % PES electrospun webs decreased to 329 nm and 215 nm, respectively, in agreement with the literature relating fiber diameter to polymer solution concentration.[41–43] The low viscosity at low solution concentration can also be one of possible causes for the beading phenomenon of the electrospun scaffold at 20 wt % PES solution (Table 1, S5) and coalescence of electrospun web at 18 wt % PES solution (Table 1, S6). The standard deviation decreased from 183 nm to 134 nm as the PES concentration decreased from 22 wt % to 18 wt % (Fig. 6) indicating that the decrease of PES concentration led to a narrower distribution of electrospun fiber diameter.

### Influence of Additives: Polyethylene Oxide (PEO) in Electrospinning of PES

Various materials can be added to the polymer solution that will affect the process and properties of nanofiber by electrospinning. Blended polymers, for instance, will retain certain properties of all polymers in the resulting fiber. During this investigation, polyethylene oxide (PEO, $M_w$ = 5000 kDa) was added into the PES solution. Even though PEO had good miscibility with PES,[44,45] PEO concentrations were kept low because of its high molecular weight, which at even moderate concentrations could greatly increase the viscosity of the solution. PEO was chosen for two reasons: (1) it could be used to enhance the hydrophilicity of PES membrane,[46] and (2) its long polymer chains might improve the spinning process by increasing the degree of polymer chain entanglement, which could reduce the beading phenomenon. The chosen tests, as shown here, utilized a

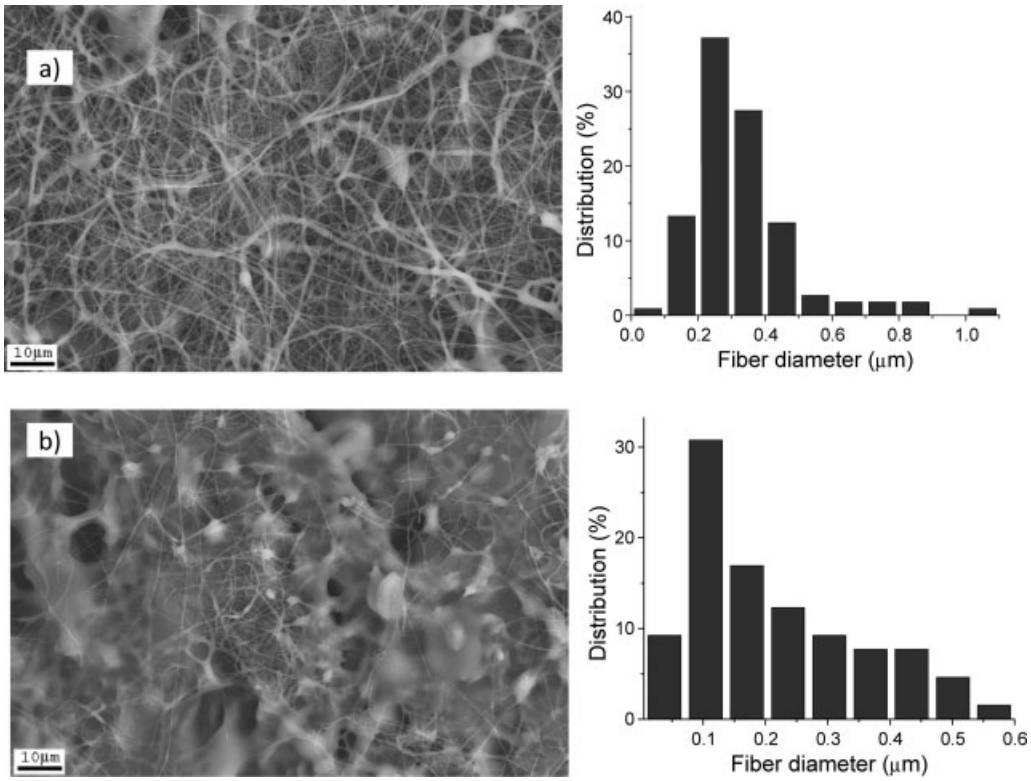


**Figure 2.** SEM images and fiber diameter distribution of electrospun Nano-PES/PET composite substrates fabricated at different PES solution concentration. Electrospinning conditions, DMF/NMP = 60/40 (wt/wt); flow rate, 20 $\mu$L/min; voltage, 30 KV; relative humidity, 50%; distance between spinneret and PET non-woven substrate, 10.5 cm; temperature, 25 °C (Table 2, no. 5–6). (a) 20 wt % PES solution, mean diameter: 329 nm. (b) 18 wt % PES solution, mean diameter: 215 nm.

0.5 wt % of PEO. Table 2 illustrates that upon addition of PEO, the nanofiber diameter increased slightly from 329 to 349 nm for a 20 wt % PES solution. The adhesion strength also increased from 34.1 to 40.2 psi (Table 2, no. 7). The high polymer concentration and correspondingly high solution viscosity could be the possible causes resulting in an increase in the fiber diameter.[42,47] Because 0.5 wt % PEO additive led to an increase of adhesion of the nano-PES/PET substrate but only affected slightly the nanofiber diameter, the 20 wt % PES solution with 0.5 wt % PEO additive was used for the electrospinning process to make a porous nano-PES/PET composite support substrate for TFNC NF membrane, whose fabrication and performance evaluation will be described elsewhere.

### Influence of Relative Humidity in Electrospinning of PES

Environmental conditions near the jet play a significant role in the elecrospinning process. The process may be quite sensitive to relative humidity (RH), especially considering that PES is precipitated by water and both chosen solvents are very hygroscopic. The presence of humidity may also change the evaporation rate of the solvent which, as we have already discussed, changes the overall adhesive quality of the nanofibers. Figure 3 shows SEM images and fiber diameter distribution of electrospun nanofiber in nano-PES/PET composite substrates fabricated under different RH. High humidity led to significantly large fibers as the fiber size increased from 266 nm at 45% RH (Table 2, no. 8) to 492 nm at 70% RH (Table 2, no. 10). This could be explained by the influence of RH on the effect of electric field. At higher humidities, more water molecules are between the spinneret and the collector. The presence of these molecules would increase the conductivity of this region, thereby changing the properties of the electric field due to the polarization of water molecules.[48] High humidity reduced the intensity of the electric field (dampening). Consequently, the electrospun fiber became thicker at high RH

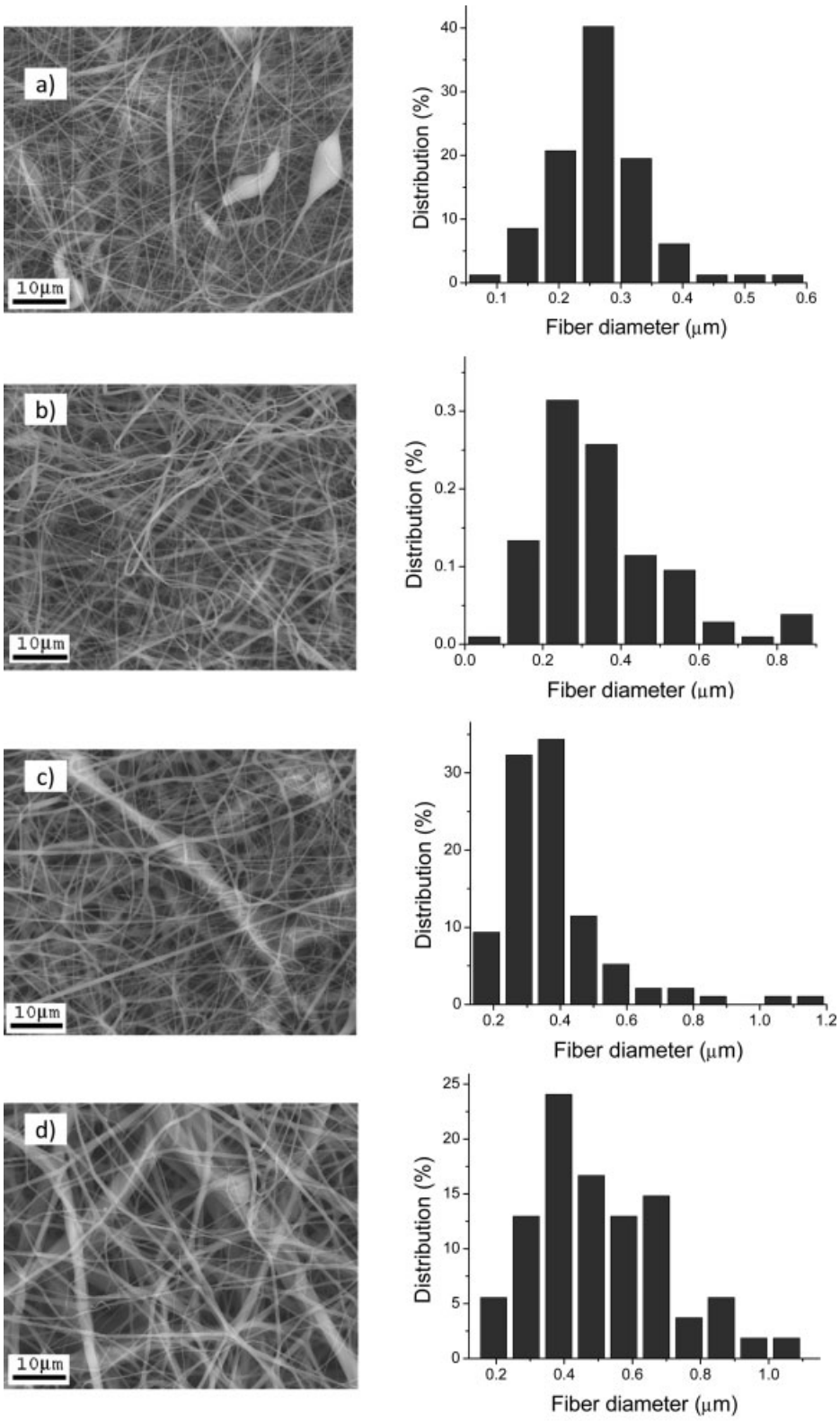


**Figure 3.** SEM images and fiber diameter distribution of electrospun Nano-PES/PET composite substrates fabricated at different relative humidity. Electrospinning conditions, DMF/NMP = 60/40 (wt/wt); 20 wt % PES; 0.5 wt % PEO; flow rate, 20 $\mu$L/min; voltage, 30 KV; distance between spinneret and PET non-woven substrate, 10.5 cm; temperature, 25 °C (Table 2, no. 7–10). (a) RH: 45%, mean diameter: 266 nm. (b) RH: 50%, mean diameter: 349 nm. (c) RH: 60%, mean diameter: 382 nm. (d) RH: 70%, mean diameter: 492 nm.

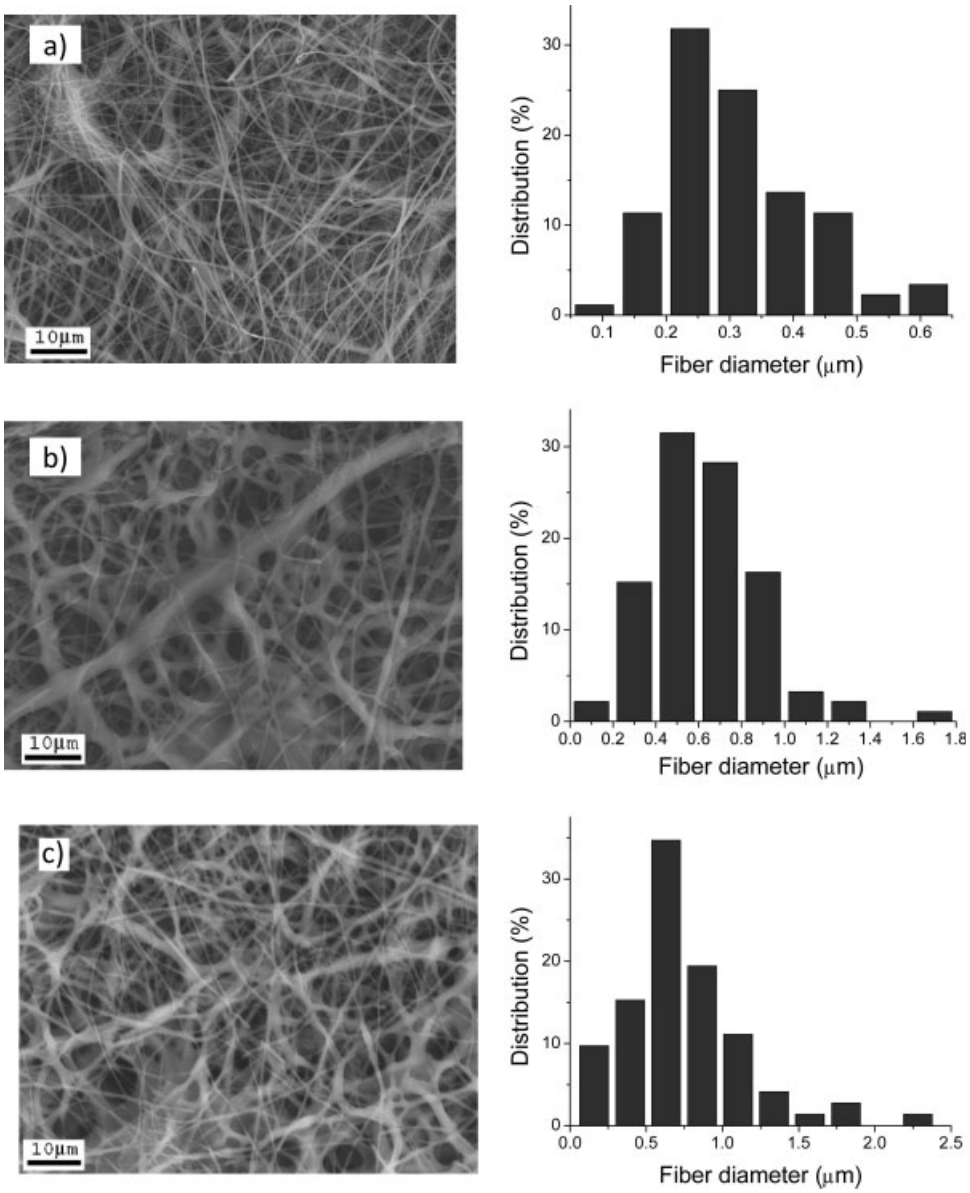


**Figure 4.** SEM images and fiber diameter distribution of electrospun Nano-PES/PET composite substrates fabricated using different flow rate. Electrospinning conditions, DMF/NMP = 60/40 (wt/wt); 20 wt % PES; 0.5 wt % PEO; relative humidity, 50%; voltage, 30 KV; distance between spinneret and PET non-woven substrate, 10.5 cm; temperature, 25 °C (Table 2, no. 11–13). (a) 15 μL/min, mean diameter: 312 nm. (b) 25 μL/min, mean diameter: 633 nm. (c) 30 μL/min, mean diameter: 740 nm.

because a thick-diameter fiber could come from a weaker applied electric field strength and hence a smaller draw-down force.[49] Another possibility is that the water molecules were diffusing into the jet causing "precipitation" of the polymer earlier in its travel pathway to the collector surface. The jet stream became thicker nearer to the spinneret and became thinner as it approached the collector surface. The standard deviation of fiber diameter also increased from 81 to 211 nm as the RH was increased from 45 to 70% (Table 2, no. 7–10), indicating that high RH could lead to a wider distribution of electrospun fiber diameter, possibly due to the instability of the jet stream in the electrospinning process caused by a combination of decreased electric field strength and

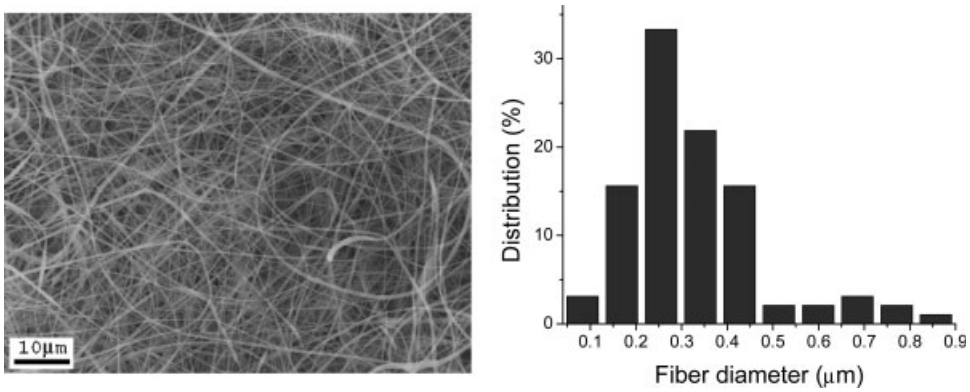


**Figure 5.** Use of "Primer Layer." Electrospinning conditions, DMF/NMP = 60/40 (wt/wt); 20 wt % PES; 0.5 wt % PEO; voltage, 30 KV; distance between spinneret and PET non-woven substrate, 10.5 cm; temperature, 25 °C; flow rate of "Primer Layer," 30 μL/min; flow rate of second layer: 15 μL/min, mean diameter: 318 nm (Table 2, no. 14).

"precipitation" of polymers within the jet before fiber deposition.

Overall RH also showed great influence on the adhesion strength between electrospun PES nanofiber and PET non-woven support. The adhesion strength was 2.6 psi when the RH was 45%. As the RH was increased to 50%, the adhesion strength increased to 40.2 psi. But with further increase in the RH to 60%, the adhesion strength decreased slightly to 32.0 psi. When the RH was increased to 70%, the adhesion strength decreased significantly to 4.70 psi (Table 2, 7–10). These results could be attributed to the formation of a PES skin layer after the jet of PES solution came into contact with the surrounding environment. The rate of skin formation should increase with an increase in humidity of the surrounding environment. The skin formation should also reduce the solvent evaporation. Therefore, when the RH was low, for example, 45%, the speed of skin formation should also be low, so the electrospun fiber had become drier when the jet fiber reached the PET non-woven support, resulting in weak adhesion strength (2.6 psi). When the RH was increased to 50%, the rate of skin formation should also be increased. So the electrospun fiber would contain a significant amount of solvent when it reached the PET non-woven support because the presence of skin could reduce the rate of solvent evaporation. As a consequence, slight coalescence of fibers appeared in the nano-PES/PET substrate at RH 50% [Fig. 3(b)] and the corresponding adhesion strength increased significantly to 40.2 psi. When the RH was further increased to 70%, more water would be absorbed during electrospinning, "precipitating" PES in the jet stream, restraining the polymer mobility and preventing coalescence of electrospun fibers [Fig. 3(d)]. Therefore, the adhesion strength significantly decreased to 4.70 psi for the nano-PES/PET composite substrate.

### Influence of Solution Flow Rate in Electrospinning of PES

The SEM images and fiber diameter distribution of electrospun PES nanofibrous scaffolds in nano-PES/PET substrates using different solution flow rate are given in Figure 4. When the solution flow rate was 15 μL/min, uniform and thin electrospun fibers were obtained. The mean diameter of electrospun fibers was 312 nm and the adhesion strength was 2.6 psi (Table 2, no. 11). As the solution flow rate was increased to 30 μL/min, the mean diameter of electrospun fiber gradually increased to 740 nm, and the adhesion strength gradually increased to 55.1 psi (Table 2, no. 13), in accordance with the literature showing that the diameter of electrospun fiber increased with increasing flow rate.[50] Wet fiber could be produced with high flow rate, as more solvent was being deposited. Therefore, it is reasonable to expect that the adhesion strength increases with increasing flow rate (Table 2, no. 10–13). The standard deviation of fiber diameter increased gradually from 112 to 408 nm as the solution flow rate was increased from 15 to 30 μL/min, showing that an increase in the solution flow rate could

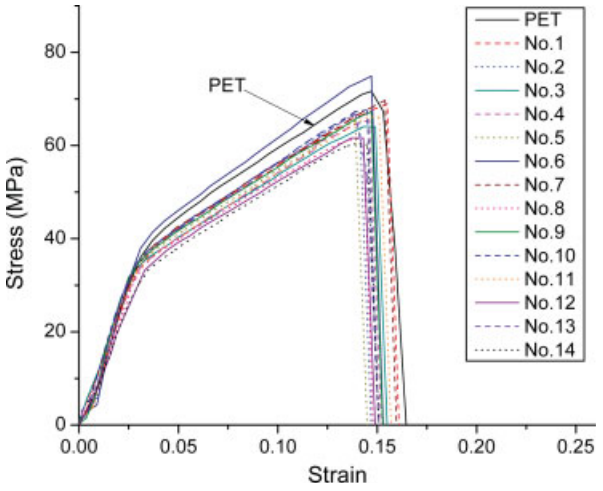


**Figure 6.** Tensile properties of PET non-woven and electrospun nano-PES/PET composite substrates. Electrospinning conditions are shown in Table 2.

widen the distribution of electrospun fiber diameter.

### Improving PES Nanofiber–PET Non-Woven Adhesion by the Use of a "Primer Layer"

Electrospun PES nanofiber with strong PET non-woven adhesion can be obtained by using a high flow rate (30 $\mu$L/min). However, these electrospun fibers are not small enough or sufficiently uniform in order to support an ultra-thin selective barrier layer in TFNC membranes. As the selective layer is usually <500 nm in thickness and the fiber diameter should be smaller in order to ensure proper support without the formation of structure defects (i.e., voids), both thin and uniform nanofibers can be obtained by using a low flow rate (15 $\mu$L/min), but unfortunately these fibers do not adhere well to the PET. Low flow rates also do not lend themselves to scale up manufacturing. We therefore implement the usage of a wet fiber deposited first as a "primer layer" before depositing the smaller, more uniform nanofibers. A uniform nanofiber top layer with 318 nm mean diameter fibers and 42.9 psi adhesion strength (Fig. 5; Table 2, no. 14) was obtained when the flow rate of the primer layer was 30 $\mu$L/min, followed by a second layer of the same solution at 15 $\mu$L/min. The fiber deposited at 30 $\mu$L/min should provide adhesive quality, whereas the fiber deposited at 15 $\mu$L/min could serve as the interface to the polyamide selective layer.

### Tensile Properties of Nano-PES/PET Composite Substrates

Figure 6 shows the results of tensile measurements of PET non-woven support and electrospun nano-PES/PET composite substrates. The stress-strain curves of electrospun nano-PES/PET composite substrates are almost the same as PET non-woven support. The values of tensile modulus, tensile strength, and elongation to break ratio of the electrospun nano-PES/PET composite substrates are also similar to that of PET non-woven substrate (Table 2). This is in accordance with our expectation that the PET non-woven support could provide the bulk of the mechanical strength of nano-PES/PET composite substrates.

## CONCLUSIONS

The critical component for fabricating high-flux TFNC membranes is to design and construct a high quality mid-layer of nanofibrous scaffold, which was demonstrated in this study. The chosen TFNC membranes involve the fabrication of PES nanofiber using electrospinning in a mixed solvent (DMF and NMP) on the PET non-woven support. The key learning points in this study can be summarized as follows:

1. Fiber diameter and its distribution are two important criteria for determining whether or not a nanofiber scaffold is suitable for supporting a thin selective barrier layer. An increase in DMF/NMP ratio, PES concentration, RH, and flow rate can result in thick PES nanofibers and a wider distribution of nanofiber diameter.
2. Adhesion between the nanofiber and the PET non-woven support was also evaluated by adjusting various processing parameters. The PES nanofiber–PET non-woven adhesion increased with an increase in DMF/NMP ratio, PES concentration, high flow rate, and the addition of PEO. PEO, however, also exhibited the added effect of slightly increasing the fiber diameter (likely due to the viscoelastic effect associated with a higher solution viscosity).
3. Overall RH showed a complicated influence on the PES nanofiber–PET non-woven adhesion. At low RH (<45%), the PES nanofiber–PET adhesion was relatively low (2.6 psi). As the RH was increased to 50%, the PES nanofiber–PET adhesion increased

significantly to 40.2 psi, possibly due to the "skin" formation, preventing the evaporation of solvent. A further increase in the RH to 70% significantly decreased the PES nanofiber–PET adhesion because of likely "precipitation" of PES in the jet stream during electrospinning.

4. A uniform nano-PES/PET composite substrate with strong PES nanofiber–PET non-woven adhesion could be obtained by using a "primer layer" coating on PET non-woven to enhance the deposit of a layer of high quality thin nanofiber (e.g., mean diameter: 329 nm; total nanofiber adhesion strength: 42.9 psi).
5. The tensile strength of nano-PES/PET composite substrate, representative to the TFNC membrane integrity, was found to be determined exclusively by the PET non-woven support and not the nanofiber layer.

This work was supported in part by Stonybrook Purification, Inc. The authors thank Robert Riley (Separation Systems Technology, Inc.) for valuable discussions.

## REFERENCES AND NOTES

1. Wang, D. X.; Wang, X. L.; Tomi, Y.; Ando, M.; Shintani, T. J Membr Sci 2006, 280, 734–743.
2. Vandezande, P.; Gevers, L. E. M.; Vankelecom, I. F. J. Chem Soc Rev 2008, 37, 365–405.
3. Hilal, N.; Al-Zoubi, H.; Darwish, N. A.; Mohammad, A. W.; Abu Arabi, M. Desalination 2004, 170, 281–308.
4. Bellona, C.; Drewes, J. E.; Xu, P.; Amy, G. Water Res 2004, 38, 2795–2809.
5. Van Der Bruggen, B.; Everaert, K.; Wilms, D.; Vandecasteele, C. J Membr Sci 2001, 193, 239–248.
6. Thanuttamavong, M.; Yamamoto, K.; Oh, J. I.; Choo, K. H.; Choi, S. J. Desalination 2002, 145, 257–264.
7. Nicoll, H. Filtr Sep 2001, 38, 22–23.
8. Eriksson, P. Environ Prog 1988, 7, 58–62.
9. Petersen, R. J. J Membr Sci 1993, 83, 81–150.
10. Liu, M. H.; Yu, S. C.; Yong, Z.; Gao, C. J. J Membr Sci 2008, 310, 289–295.
11. Zhang, S. H.; Jian, X. G.; Dai, Y. J Membr Sci 2005, 246, 121–126.
12. Mohammad, A. W.; Hilal, N.; Abu Seman, M. N. Desalination 2003, 158, 73–78.
13. Song, Y. J.; Liu, F.; Sun, B. H. J Appl Polym Sci 2005, 95, 1251–1261.
14. Kim, I. C.; Jegal, J.; Lee, K. H. J Polym Sci Part B: Polym Phys 2002, 40, 2151–2163.
15. Razdan, U.; Kulkarni, S. S. Desalination 2004, 161, 25–32.
16. Zhang, Y. F.; Xiao, C.; Liu, E. H.; Du, Q. Y.; Wang, X.; Yu, H. L. Desalination 2006, 191, 291–295.
17. Lu, X. F.; Bian, X. K.; Shi, L. Q. J Membr Sci 2002, 210, 3–11.
18. Buch, P. R.; Mohan, D. J.; Reddy, A. V. R. Polym Int 2006, 55, 391–398.
19. Oh, N. W.; Jegal, J.; Lee, K. H. J Appl Polym Sci 2001, 80, 2729–2736.
20. Oh, N. W.; Jegal, J.; Lee, K. H. J Appl Polym Sci 2001, 80, 1854–1862.
21. Korikov, A. R.; Kosaraju, R.; Sirkar, K. K. J Membr Sci 2006, 279, 588–600.
22. Gevers, L. E. M.; Aldea, S.; Vankelecom, I. F. J.; Jacobs, P. A. J Membr Sci 2006, 281, 741–746.
23. Kuehne, M. A.; Song, R. Q.; Li, N. N.; Petersen, R. J. Environ Prog 2001, 20, 23–26.
24. Lang, K.; Sourirajan, S.; Matsuura, T.; Chowdhury, G. Desalination 1996, 104, 185–196.
25. Richard, W. B. Membrane Technology and Applications; 2nd ed.; John Wiley & Sons Ltd: Chichester, UK, 2004; pp 89–160.
26. Heikkila, P.; Taipale, A.; Lehtimaki, M.; Harlin, A. Polym Eng Sci 2008, 48, 1168–1176.
27. Nakata, K.; Kim, S. H.; Ohkoshi, Y.; Gotoh, Y.; Nagura, M. Sen-I Gakkash 2007, 63, 307–312.
28. Qin, X. H.; Wang, S. Y. J Appl Polym Sci 2006, 102, 1285–1290.
29. Li, W. J.; Laurencin, C. T.; Caterson, E. J.; Tuan, R. S.; Ko, F. K. J Biomed Mater Res 2002, 60, 613–621.
30. Gopal, R.; Kaur, S.; Feng, C. Y.; Chan, C.; Ramakrishna, S.; Tabe, S.; Matsuura, T. J Membr Sci 2007, 289, 210–219.
31. Wang, X. F.; Chen, X. M.; Yoon, K.; Fang, D. F.; Hsiao, B. S.; Chu, B. Environ Sci Technol 2005, 39, 7684–7691.
32. Wang, X. F.; Fang, D. F.; Yoon, K.; Hsiao, B. S.; Chu, B. J Membr Sci 2006, 278, 261–268.
33. Yoon, K.; Kim, K.; Wang, X. F.; Fang, D. F.; Hsiao, B. S.; Chu, B. Polymer 2006, 47, 2434–2441.
34. Yoon, K.; Hsiao, B. S.; Chu, B. J Membr Sci 2008, 326, 484–492.
35. Luo, M. L.; Zhao, J. Q.; Tang, W.; Pu, C. S. Appl Surf Sci 2005, 249, 76–84.
36. Idris, A.; Zain, N. M.; Noordin, M. Y. Desalination 2007, 207, 324–339.
37. Vane, L. M.; Rodriguez, F. J Appl Polym Sci 1993, 49, 765–776.
38. Howard, P. H. Handbook of Environmental Fate and Exposure Data for Organic Chemicals; CRC: Boca Raton, FL, 1993.
39. Lee, K. P.; Chromey, N. C.; Culik, R.; Barnes, J. R.; Schneider, P. W. Fundam Appl Toxicol 1987, 9, 222–235.
40. Bancroft, W. D.; Davis, H. L. J Phys Chem 1929, 33, 361–370.

41. He, J. H.; Wan, Y. Q.; Yu, J. Y. Fiber Polym 2008, 9, 140–142.
42. Yamshita, Y.; Ko, F.; Tanaka, A.; Miyake, H. J Text Eng 2007, 53, 137–142.
43. Deitzel, J. M.; Kleinmeyer, J.; Harris, D.; Tan, N. C. B. Polymer 2001, 42, 261–272.
44. Genix, A. C.; Arbe, A.; Arrese-Igor, S.; Colmenero, J.; Richter, D.; Frick, B.; Deen, P. P. J Chem Phys 2008, 128, 184901-1–184901-11.
45. Dreezen, G.; Fang, Z.; Groeninckx, G. Polymer 1999, 40, 5907–5917.
46. Yamanouchi, D.; Wu, J.; Lazar, A. N.; Craig Kent, K.; Chu, C.-C.; Liu, B. Biomaterials 2008, 29, 3269–3277.
47. Lin, Y.; Yao, Y. Y.; Yang, X. Z.; Wei, N.; Li, X. Q.; Gong, P.; Li, R. X.; Wu, D. C. J Appl Polym Sci 2008, 107, 909–917.
48. Medeiros, E. S.; Mattoso, L. H. C.; Offeman, R. D.; Wood, D. F.; Orts, W. J. Can J Chem 2008, 86, 590–599.
49. Wang, C.; Hsu, C. H.; Lin, J. H. Macromolecules 2006, 39, 7662–7672.
50. Fridrikh, S. V.; Yu, J. H.; Brenner, M. P.; Rutledge, G. C. Phys Rev Lett 2003, 90, 144502-1–144502-4.